J|A|C|S
ARTICLES
Published on Web 10/23/2004

Dynamics and Mechanisms of the Multiphoton Gated Photochromic Reaction of Diarylethene Derivatives

Masataka Murakami,[†] Hiroshi Miyasaka,*[,†] Tadashi Okada,[†] Seiya Kobatake,[‡] and Masahiro Irie*[,‡]

Contribution from the Division of Frontier Materials Science, Graduate School of Engineering Science, and Research Center of Materials Science at Extreme Conditions, Osaka University, Toyonaka, Osaka 560-8531, Japan, and Department of Chemistry and Biochemistry, Graduate School of Engineering, Kyushu University, Hakozaki 6-10-1, Higashi-ku, Fukuoka 812-8581, Japan

Received February 14, 2004; E-mail: miyasaka@chem.es.osaka-u.ac.jp; irie@cstf.kyushu-u.ac.jp

Abstract: The cycloreversion (ring-opening) process of one of the photochromic diarylethene derivatives, bis(2-methyl-5-phenylthiophen-3-yl)perfluorocyclopentene, was investigated by means of picosecond and femtosecond laser photolysis methods. The drastic enhancement of the reaction yield was observed only by the picosecond laser exposure. The excitation intensity effect of the reaction profiles revealed that the successive multiphoton absorption process leading to higher excited states opened the efficient cycloreversion process with a reaction yield of (50 ± 10)%, while the one-photon absorption directly pumped to a higher excited state did not lead to the efficient cycloreversion reaction. These results indicate that not the energy of the excitation but the character of the electronic state takes an important role in the enhancement of the cycloreversion reaction.

Introduction

Photochromism is a photoinduced reversible isomerization in a chemical species between two forms. The instant property change arising from the chemical-bond reconstruction via photoexcitation has been attracting much attention not only from the viewpoint of the fundamental chemical reaction processes but also from the viewpoint of the application to optoelectronic devices such as rewritable optical memory and switches.[1−13]

Among various photochromic molecules, diarylethenes with heterocyclic aryl rings have been developed as a new type of thermally stable and fatigue-resistant photochromic compound.[3−7] Both isomers of the diarylethenes differ from each other not only in their absorption spectra, but also in various physical and chemical properties such as fluorescence spectra,[8] refractive indices,[9] oxidation/reduction potentials,[10] and chiral properties.[11] When radicals are located at both ends of the diarylethene derivatives, the intramolecular magnetic interaction between their radicals can be controlled upon irradiation with UV and visible light.[12] The light emission control via photochromic reactions has recently provided novel functions in single molecular devices.[8a] In addition, the photochromic reaction can take place even in the crystalline phase.[13] Direct detection of the reaction dynamics revealed that most of these photochromic reactions take place in the time region ≤10 ps.[14−27]

[†] Osaka University.
[‡] Kyushu University.

(1) (a) Dürr, H.; Bouas-Laurent, H. *Photochromism Molecules and Systems*; Elsevier: Amsterdam, 1990. (b) Brown, C. H. *Photochromism*; Wiley-Interscience: New York, 1971.
(2) (a) *Molecular Switches*; Feringa, B. L., Ed.; Wiley-VCH: Weinheim, 2001. (b) Themetic issue on "Photochromism: Memories and Switches". *Chem. Rev.* **2000**, *100*, issue 5. (c) *Photoreactive Materials for Ultrahigh-Density Optical Memory*; Irie, M., Ed.; Elsevier: Amsterdam, 1994.
(3) (a) Irie, M. *Chem. Rev.* **2000**, *100*, 1685. (b) Irie, M.; Uchida, K. *Bull. Chem. Soc. Jpn.* **1998**, *71*, 985. (c) Hanazawa, M.; Sumiya, R.; Horikawa, Y.; Irie, M. *J. Chem. Soc., Chem. Commun.* **1992**, 206. (d) Irie, M.; Mohri, M. *J. Org. Chem.* **1988**, *53*, 803.
(4) (a) Fernandez-Acebes, A.; Lehn, J.-M. *Chem.-Eur. J.* **1999**, *5*, 3285. (b) Tsivgoulis, G. M.; Lehn, J.-M. *Angew. Chem., Int. Ed. Engl.* **1995**, *34*, 1119. (c) Gilat, S. L.; Kawai, S. H.; Lehn, J.-M. *J. Chem. Soc., Chem. Commun.* **1993**, 1439.
(5) (a) Lucas, L. N.; de Jong, J. J. D.; van Esch, J. H.; Kellogg, R. M.; Feringa, B. L. *Eur. J. Org. Chem.* **2003**, 155. (b) Feringa, B. L.; Jager, W. F.; Delange, B. *Tetrahedron* **1993**, *49*, 8267.
(6) (a) Peters, A.; Branda, N. R. *J. Am. Chem. Soc.* **2003**, *125*, 3404. (b) Myles, A. J.; Branda, N. R. *Adv. Funct. Mater.* **2002**, *12*, 167. (c) Murguly, E.; Norsten, T. B.; Branda, N. R. *Angew. Chem., Int. Ed.* **2001**, *40*, 1752.
(7) (a) Luo, Q.; Chen, B.; Wang, M.; Tian, H. *Adv. Funct. Mater.* **2003**, *13*, 233. (b) Yokoyama, Y.; Shiraishi, H.; Tani, Y.; Yokoyama, Y.; Yamaguchi, Y. *J. Am. Chem. Soc.* **2003**, *125*, 7194. (c) Uchida, K.; Saito, M.; Murakami, A.; Nakamura, S.; Irie, M. *ChemPhysChem* **2003**, *4*, 1124. (d) Bertarelli, C.; Gallazzi, M. C.; Stellacci, F.; Zerbi, G.; Stagira, S.; Nisoli, M.; De Silvestri, S. *Chem. Phys. Lett.* **2002**, *359*, 278. (e) Cho, H.; Kim, E. *Macromolecules* **2002**, *35*, 8684.
(8) (a) Irie, M.; Fukaminato, T.; Sasaki, T.; Tamai, N.; Kawai, T. *Nature* **2002**, *420*, 759. (b) Kawai, T.; Sasaki, T.; Irie, M. *Chem. Commun.* **2001**, 711. (c) Norsten, T. B.; Branda, N. R. *J. Am. Chem. Soc.* **2001**, *123*, 1784. (d) Takeshita, M.; Irie, M. *Chem. Lett.* **1998**, 1123. (e) Takeshita, M.; Soong, C.-F.; Irie, M. *Tetrahedron Lett.* **1998**, *39*, 7717.
(9) (a) Chauvin, J.; Kawai, T.; Irie, M. *Jpn. J. Appl. Phys.* **2001**, *40*, 2518. (b) Kawai, T.; Fukuda, N.; Gröschl, D.; Kobatake, S.; Irie, M. *Jpn. J. Appl. Phys.* **1999**, *38*, L1194.
(10) (a) Gilat, S. L.; Kawai, S. H.; Lehn, J.-M. *Chem.-Eur. J.* **1995**, *1*, 275. (b) Kawai, T.; Kunitake, T.; Irie, M. *Chem. Lett.* **1999**, 905.
(11) (a) Yamamoto, S.; Matsuda, K.; Irie, M. *Angew. Chem., Int. Ed.* **2003**, *42*, 1636. (b) Kodani, T.; Matsuda, K.; Yamada, T.; Kobatake, S.; Irie, M. *J. Am. Chem. Soc.* **2000**, *122*, 9631. (c) Yamaguchi, T.; Uchida, K.; Irie, M. *J. Am. Chem. Soc.* **1997**, *119*, 6066.
(12) (a) Matsuda, K.; Matsuo, M.; Mizoguti, S.; Higashiguchi, K.; Irie, M. *J. Phys. Chem. B* **2002**, *106*, 11218. (b) Matsuda, K.; Irie, M. *J. Am. Chem. Soc.* **2001**, *123*, 9896. (c) Matsuda, K.; Irie, M. *Chem.-Eur. J.* **2001**, *7*, 3466. (d) Matsuda, K.; Irie, M. *J. Am. Chem. Soc.* **2000**, *122*, 8309.
(13) (a) Morimoto, M.; Kobatake, S.; Irie, M. *Chem. Rec.* **2004**, *4*, 23. (b) Kobatake, S.; Irie, M. *Bull. Chem. Soc. Jpn.* **2004**, *77*, 195. (c) Irie, M.; Kobatake, S.; Horichi, M. *Science* **2001**, *291*, 1769. (d) Irie, M.; Lifka, T.; Kobatake, S.; Kato, N. *J. Am. Chem. Soc.* **2000**, *122*, 4871. (e) Kobatake, S.; Yamada, T.; Uchida, K.; Kato, N.; Irie, M. *J. Am. Chem. Soc.* **1999**, *121*, 2380.
(14) Miyasaka, H.; Araki, S.; Tabata, A.; Nobuto, T.; Mataga, N.; Irie, M. *Chem. Phys. Lett.* **1994**, *230*, 249.

10.1021/ja049177+ CCC: $27.50 **© 2004 American Chemical Society**

The photochromic systems for the actual application, in general, require several conditions such as (a) thermal stability of both isomers, (b) low fatigue, (c) rapid response, (d) high sensitivity, and (e) nondestructive readout capability. Because the reaction in the excited state generally takes place in competition with various processes in a finite lifetime, the large rate constant of the photochromic reaction (the quick response) is of crucial importance for an increase in the reaction yield (the high sensitivity) and a decrease in undesirable side reactions resulting in low durability (the low fatigue). On the other hand, the nondestructive read-out capability is in conflict with the above properties, fulfilling conditions (b)−(d). Hence, the introduction of gated-function is required for the photochromic systems with nondestructive capability while reading-out by the absorption of the light. Recently, we reported multiphoton-induced enhancement of a cycloreversion reaction in photochromic diarylethene derivatives.[23,24] This multiphoton-gated reaction may provide a new approach to erasable memory media with nondestructive readout capability. Not only from the viewpoint of the application but also from the basic viewpoints of photochemistry, the selective excitation to a specific electronic state leading to the target reaction seems to provide a novel approach for the control of the photochemical reactions.

To explore the precise and quantitative information on the dynamics and mechanisms of the multiphoton photochromic reactions, we have investigated the reaction profiles dependent on the laser excitation intensity, excitation wavelength, and laser pulse durations in the present work. On the basis of these experimental results and numerical simulations, it was revealed that not the energy of the excitation but the character of the electronic state plays an important role in the multiphoton photocycloreversion process.

Experimental Section

A picosecond laser photolysis system with a repetitive mode-locked Nd^{3+}:YAG laser was used for transient absorption spectral measurements.[28,29] The second harmonic (532 nm) with 15 ps fwhm and 0.5−1 mJ was used for excitation. The excitation pulse was focused into a spot with a diameter of ca. 1.5 mm. Picosecond white continuum generated by focusing a fundamental pulse into a 10 cm quartz cell containing a D_2O and H_2O mixture (3:1) was employed as a monitoring light. A sample cell with 2 mm optical length cell was used for the 532 nm excitation. The sample solution was circulated during the measurement under the repetition rate <0.1 Hz, and the data were obtained only with one-shot laser exposure for each spectrum.

For the measurement of the dependence of the transient absorption spectra on the excitation intensity of the picosecond laser pulse, a pinhole with a diameter of 1.1 mm was placed before the sample solution. The intensity of the picosecond laser light transmitted through the sample cuvette was measured by a laser power meter (Gentec, ED-200). The reflection of the incident light at the surface of the cuvette was calibrated by the measurement of the cuvette containing only the solvent.

To investigate the dynamic behavior under femtosecond laser light excitation, a dual OPA laser system for kinetic transient absorption measurements was used.[24] The output of a femtosecond Ti:Sapphire laser (Tsunami, Spectra-Physics) pumped by the SHG of a cw Nd^{3+}:YVO_4 laser (Millennia V, Spectra-Physics) was regeneratively amplified with a 1 kHz repetition rate (Spitfire, Spectra-Physics). The amplified pulse (1 mJ/pulse energy and 85 fs fwhm) was divided into two pulses with the same energy (50%). These pulses are guided into two OPA systems (OPA-800, Spectra-Physics), respectively. OPA output pulses are converted to the SHG, THG, FHG, or sum frequency mixing with a fundamental 800 nm pulse. These pulses can cover the wavelength region between 300 and 1200 nm with 1−10 mW output energy and ca. 120 fs fwhm. One of these two pulses was used as a pump light, and the other one which is reduced to <1/5000 output power was utilized as a monitoring light. The pulse duration was estimated to be 150 fs from the cross correlation trace at the sample position. The intensities of the monitoring, reference, and pump beams were monitored by photodiode detectors and sent to the microcomputer for further analysis. The sample cell with 2 mm optical length was used, and the sample solution was circulated.

For the nanosecond transient absorption spectroscopy, SHG (532 nm) or FHG (266 nm) of the nanosecond YAG laser (Quanta Ray, DCR3) with ca. 1 mJ output power and 5 ns pulse width was used as excitation light. The combination use of the Xe lamp as a monitoring light with the diode array detector with a gated image intensifier (Hamamatsu, PMA-50) provides the transient absorption spectra with ca. 10 ns temporal resolution.

Bis(2-methyl-5-phenylthiophen-3-yl)perfluorocyclopentene, **1**, was synthesized and purified.[13d] This molecule undergoes the photochromic reactions between the open-isomer and the closed-isomer as shown in Scheme 1. *n*-Hexane (Wako, infinity pure grade) was used without further purification. All of the measurements were performed under O_2-free conditions at 22 ± 2 °C.

Scheme 1

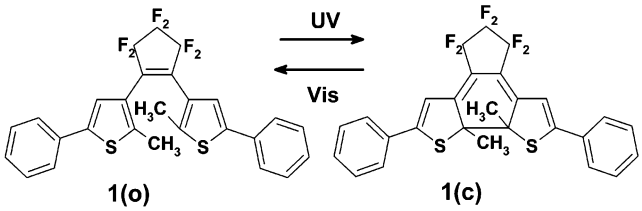

Results and Discussion

Steady-State Absorption Spectra. Figure 1 shows the ground-state absorption spectra of **1** in *n*-hexane solution. The closed-form of **1**, **1(c)**, has the absorption maximum at 585 nm in the visible region, together with peaks at 305 and 380 nm in the UV region. On the other hand, the open-form of **1**, **1(o)**, has the absorption only in the UV region. The quantum yield of the cyclization reaction from **1(o)** to **1(c)** was 0.59, whereas the quantum yield of the cycloreversion reaction leading to the **1(o)** production from **1(c)** was 0.013.[13d]

(15) Tamai, N.; Saika, T.; Shimidzu, T.; Irie, M. *J. Phys. Chem*. **1996**, *100*, 4689.
(16) Miyasaka, H.; Nobuto, T.; Itaya, A.; Tamai, N.; Irie, M. *Chem. Phys. Lett.* **1997**, *269*, 281.
(17) Ern, J.; Bens, A. T.; Bock, A.; Martin, H.-D.; Kryschi, C. *J. Lumin*. **1998**, *76 & 77*, 90.
(18) Ern, J.; Bens, A. T.; Martin, H.-D.; Mukamel, S.; Schmid, D.; Tretiak, S.; Tsiper, E.; Kryschi, C. *Chem. Phys.* **1999**, *246*, 115.
(19) Ern, J.; Bens, A. T.; Martin, H.-D.; Mukamel, S.; Tretiak, S.; Tsyganenko, K.; Kuldova, K.; Trommsdorff, H. P.; Kryschi, C. *J. Phys. Chem. A* **2001**, *105*, 1741.
(20) Ern, J.; Bens, A. T.; Martin, H.-D.; Kuldova, K.; Trommsdorff, H. P.; Kryschi, C. *J. Phys. Chem. A* **2002**, *106*, 1654.
(21) Tamai, N.; Miyasaka, H. *Chem. Rev*. **2000**, *100*, 1875.
(22) Miyasaka, H.; Nobuto, T.; Murakami, M.; Itaya, A.; Tamai, N.; Irie, M. *J. Phys. Chem. A* **2002**, *106*, 8096.
(23) Miyasaka, H.; Murakami, M.; Itaya, A.; Guillaumont, D.; Nakamura, S.; Irie, M. *J. Am. Chem. Soc.* **2001**, *123*, 753.
(24) Miyasaka, H.; Murakami, M.; Okada, T.; Nagata, Y.; Itaya, A.; Kobatake, S.; Irie, M. *Chem. Phys. Lett.* **2003**, *371*, 40.
(25) Hania, P. R.; Telesca, R.; Lucas, L. N.; Pugzlys, A.; van Esch, J.; Feringa, B. L.; Snijders, J. G.; Duppen, K. *J. Phys. Chem. A* **2002**, *106*, 8498.
(26) Okabe, C.; Nakabayashi, T.; Nishi, N.; Fukaminato, T.; Kawai, T.; Irie, M.; Sekiya, H. *J. Phys. Chem. A* **2003**, *107*, 5384.
(27) Shim, S.; Joo, T.; Bae, S. C.; Kim, K. S.; Kim, E. *J. Phys. Chem. A* **2003**, *107*, 8106.
(28) Miyasaka, H.; Moriyama, T.; Kotani, S.; Muneyasu, R.; Itaya, A. *Chem. Phys. Lett*. **1994**, *225*, 315.
(29) Miyasaka, H.; Moriyama, T.; Itaya, A. *J. Phys. Chem.* **1996**, *100*, 12609.

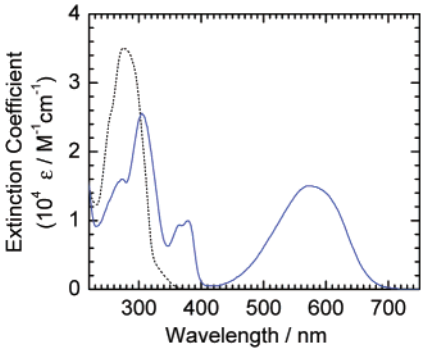

Figure 1. Absorption spectra of the closed-ring isomer of **1**, **1(c)** (blue smooth line), and the open-ring isomer, **1(o)** (black dotted line), in the S_0 state in *n*-hexane solution.

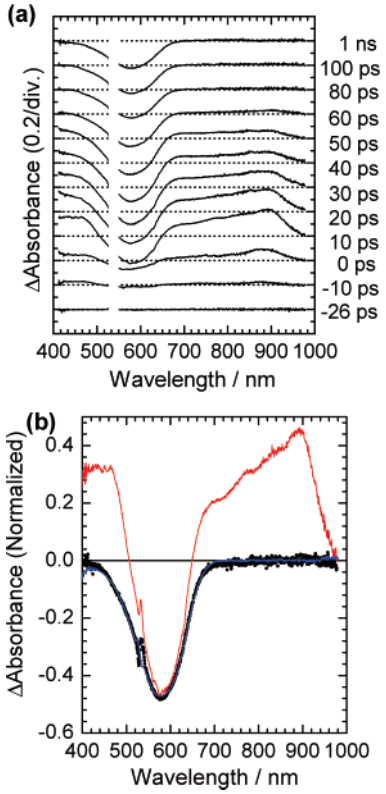

Figure 2. (a) Time-resolved transient absorption spectra of **1(c)** in *n*-hexane, excited with a 15 ps fwhm, 532 nm laser pulse with 0.4 mJ/mm^2 output power. (b) Transient absorption spectra of **1(c)** in *n*-hexane normalized at 590 nm, observed at 10 ps (red line) and 100 ps (●) after the excitation. The blue solid line is a negative image of the ground-state absorption of **1(c)**.

Picosecond Laser Photolysis and Transient Absorption Spectroscopy of the Cycloreversion Reaction. Figure 2a shows the time-resolved transient absorption spectra of **1(c)** in *n*-hexane solution, excited with a picosecond 532 nm laser pulse. An excitation intensity of 0.4 mJ/mm^2 was employed for the spectral measurements. A negative absorption band with a maximum at 585 nm and positive absorption bands in the wavelength regions longer than 650 nm and shorter than 450 nm appear immediately after the excitation. The former negative absorption can be safely ascribed to the bleaching signal of the ground state **1(c)**. On the other hand, the positive absorption bands are assigned to the excited state of **1(c)** because the decay time constant was in agreement with that for the recovery of the former bleaching signal as will be shown in later. At and after 80 ps following the excitation, almost all positive absorption signals disappeared and constant negative absorption remained. As shown in Figure 2b, the transient absorption spectrum at 100 ps after the excitation was identical with the negative image of the ground-state absorption spectrum. In addition, this negative absorption spectrum was observed even at several seconds after the excitation without circulation of the sample and the ground-state spectrum covering the UV region consisted of only **1(o)** and **1(c)**. The UV light irradiation after several hundred shots of the picosecond laser pulse perfectly recovered the absorbance of **1(c)**. Hence, this negative absorption signal as observed in the transient absorption spectra at and after 80 ps following the excitation was assigned to the cycloreversion reaction from **1(c)** to **1(o)**. Summarizing the above results and discussion, the cycloreversion reaction with no remarkable subreaction completed within several tens of picoseconds following the excitation.

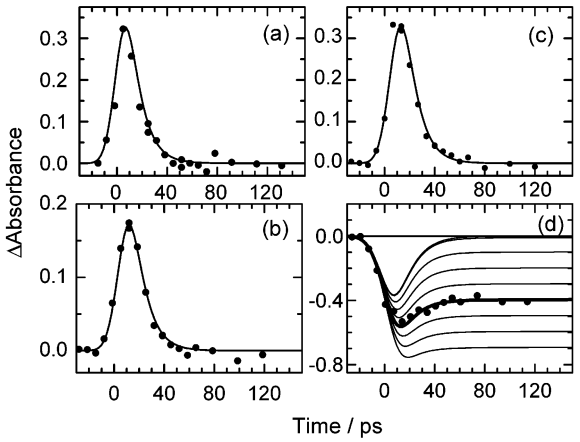

Figure 3. Time profiles of the transient absorbance of **1(c)** in *n*-hexane, excited with a 15 ps fwhm, 532 nm laser pulse with 0.4 mJ/mm^2 output power, and observed at 440 nm (a), 710 nm (b), 890 nm (c), and 580 nm (d). Solid lines are convolution curves calculated on the basis of the pulse widths of pump and probe pulse (15 ps) and a time constant (10 ps). The lines in (d) are the results calculated with the reaction yield as a parameter. From the top, the reaction yields of 0, 0.01, 0.1, 0.2, 0.3, 0.4, 0.5, 0.6, and 0.7 were respectively set for the calculation with the pulse width of 15 ps and the time constant of 10 ps. The bold line with the reaction yield of 0.4 best reproduces the experimental result in (d) (see text).

Figure 3 shows the time profiles of **1(c)** in *n*-hexane solution monitored at several wavelength points following the picosecond 532 nm laser excitation with 0.4 mJ/mm^2 output power. The time profiles at 440, 710, and 890 nm show the rapid appearance of the positive absorbance followed by the decay in several tens of picoseconds time region. The solid lines in Figure 3a−c are curves calculated on the basis of the pulse widths of the exciting and monitoring pulses and the decay time constant. In this calculation, the monophasic decay with a time constant of 10 ps was assumed. This figure shows that curves thus calculated reproduce the experimental results well. On the other hand, the time profile at 580 nm shows that the negative transient absorbance appearing within the response of the apparatus recovers slightly in several tens of picoseconds time region, followed by the constant negative value due to the cycloreversion process from **1(c)** to **1(o)**.

For the analysis of the time profile at 580 nm, we tentatively assumed the simple reaction scheme that the excited state of **1(c)** undergoes deactivation into the ground state in competition with the cycloreversion reaction leading to the **1(o)** production as shown in Scheme 2, where the reaction yield of the cyclo-

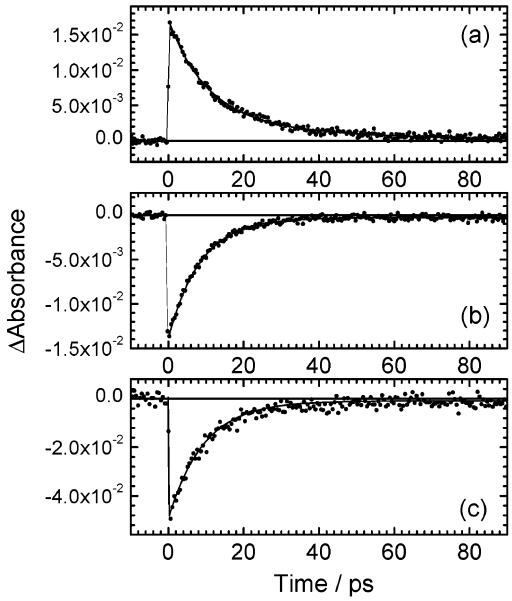

Figure 4. Time profiles of the transient absorbance of **1(c)** in *n*-hexane, excited with a 150 fs fwhm laser pulse; (a) excited at 580 nm and monitored at 680 nm, (b) excited at 580 nm and monitored at 620 nm, and (c) excited at 540 nm and monitored at 580 nm. Solid lines are calculated curves by taking into account the pulse durations, the time constant, and the reaction yield.

Scheme 2

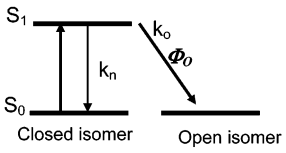

reversion reaction, Φ_o, is represented as $k_o/(k_n + k_o)$. Here, k_n and k_o are respectively the rate constant of the deactivation into the ground state and that of the cycloreversion reaction. In the analysis, $1/(k_n + k_o)$ was set to the decay time constant of the positive absorption signals of 10 ps. Solid lines in Figure 3d are the curves calculated with various Φ_o values. This figure indicates that the experimental result is well reproduced with $\Phi_o = 40\%$, although the quantum yield of the **1(c)** to **1(o)** in *n*-hexane solution was obtained to be 1.3% under steady-state irradiation.[13d]

Femtosecond Laser Photolysis and Dynamics of the Cycloreversion Reaction. Prior to the discussion on the enhancement of the cycloreversion reaction yield, we show the dynamic behaviors under femtosecond laser pulse excitation. In Figure 4 are exhibited the time profiles of **1(c)** in *n*-hexane solution excited with a femtosecond laser pulse. The time profile monitored at 680 nm following the excitation at 580 nm shows the rapid appearance of the positive absorption due to the excited state, followed by the monophasic decay with a time constant of 9.8 ± 0.6 ps. At the monitoring wavelength of 620 nm (Figure 4b), the quick appearance of the negative absorption signal due to the bleaching of the ground state **1(c)** was followed by the recovery in several tens of picoseconds time region. This timeprofile was reproduced also by a single-exponential function with the time constant of 9.6 ± 1.0 ps. The residual signal (1−2%) at and after several tens of picoseconds following the excitation is ascribable to the conversion of **1(c)** to **1(o)**. Actually, the residual signal did not decrease in the time window

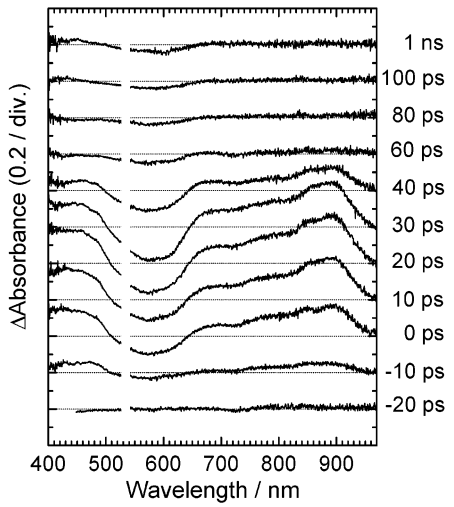

Figure 5. Time-resolved transient absorption spectra of **1(c)** in *n*-hexane, excited with a 15 ps fwhm, 532 nm laser pulse with 0.06 mJ/mm^2 output power.

available in this measurement (ca. 3 ns), and the yield was almost identical to the cycloreversion quantum yield of **1(c)** obtained by the steady-state irradiation.[13d]

The excitation energy dependence of the reaction profile under the femtosecond laser pulse exposure was investigated by changing the pump laser wavelength. Figure 4c shows the time profile monitored at 580 nm following the 540 nm laser excitation. The quick appearance of the negative absorption was followed by the monophasic decay with a time constant of 9.6 ± 1.5 ps. The residual signal at and after several tens of picoseconds following the excitation was also estimated to be 1−2%. In the excitation wavelength region of 540−620 nm, no remarkable difference of the recovery time constant and the residual signal due to the cycloreversion reaction was observed, indicating that the drastic enhancement of the cycloreversion yield under picosecond laser excitation was not due to the vibrational excess energy in the excited state attained by the excitation of the visible band of **1(c)**.

Excitation Intensity Dependence of the Cycloreversion Reaction Dynamics under Picosecond Laser Excitation. To explore the large enhancement of the cycloreversion reaction yield under the picosecond 532 nm laser excitation, the excitation intensity dependence of the reaction dynamics was investigated. Figure 5 shows transient absorption spectra of **1-(c)** in *n*-hexane solution excited with a picosecond laser pulse with an excitation intensity of 0.06 mJ/mm^2. The transient absorption spectra immediately after the excitation show a negative absorption band centered at 585 nm and the positive absorption signal with a maximum at 880 nm and that in the wavelength region shorter than 500 nm, as observed in Figure 2 with much higher excitation intensity. With an increase in the delay time after the excitation, these positive and negative absorption bands decrease in several tens of picoseconds time region. No remarkable time evolution was observed at and after 80 ps following the excitation, and the residual negative absorption safely assigned to the cycloreversion reaction leading to the production of **1(o)** was also detected. In addition, the time constants of the decay and the recovery were 10 ps, which was the same as that obtained for the high excitation condition. Comparison of the residual intensity in longer delay time,

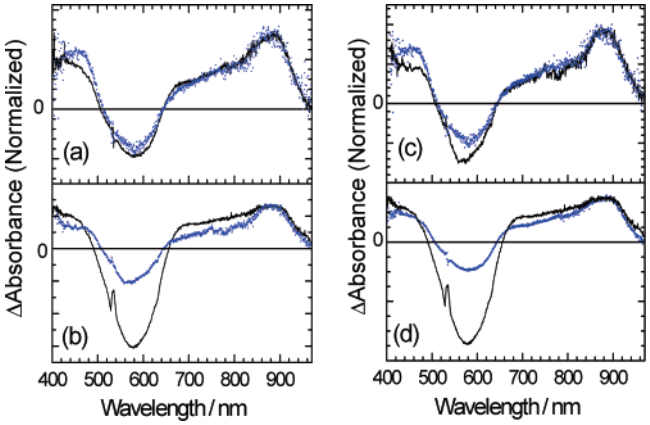

Figure 6. Excitation intensity effect of the 15 ps 532 nm laser pulse on the transient absorption spectra of **1(c)** in *n*-hexane solution. The incident energies of 0.4 mJ/mm^2 (the higher) and 0.06 mJ/mm^2 were employed. (a) Absorption spectra observed at 0 ps (blue dotted line) and at 30 ps (black solid line) after the excitation with the lower output power. (b) Absorption spectra observed at 0 ps (blue dotted line) and at 30 ps (black solid line) after the higher excitation intensity. (c) Spectra observed at 0 ps after the excitation with the lower excitation intensity (blue dotted line) and with the higher one (black solid line). (d) Spectra observed at 30 ps after the excitation with the lower excitation intensity (blue dotted line) and with the higher intensity (black solid line). All of the spectra were normalized at 880 nm.

however, clearly indicates that a much weaker residual signal relative to the positive absorption in the early stage after the excitation was obtained in Figure 5. This result indicates that some nonlinear processes are responsible for the enhancement of the cycloreversion under picosecond excitation as observed in Figure 2.

Not only were the spectra dependent on the cycloreversion yield as a remaining absorption signal, transient absorption spectra immediately after the excitation were also dependent on the excitation intensity as shown in Figure 6, where the spectra were normalized at the positive absorption maximum at 880 nm. One can easily find several characteristic differences of the spectra in Figure 6. First, we discuss the time evolution of the transient spectra under the lower excitation condition with 0.06 mJ/mm^2. Figure 6a shows the normalized absorption spectra observed at 0 and 30 ps after the excitation, indicating that the positive absorption band shape is almost independent of the delay time and the negative absorption signal in the spectrum at 30 ps after the excitation is slightly larger than that at 0 ps. The slightly larger contribution of the negative absorption in the spectrum at 30 ps is attributable to the production of the open isomer in longer delay time. On the other hand, the normalized absorption spectra observed at 0 and 30 ps after the excitation with the higher energy (0.4 mJ/mm^2) in Figure 6b shows a remarkable difference. The intensity of the negative absorption with a maximum at 585 nm at 30 ps is much larger than that at 0 ps. In addition, one can find the difference in the spectral band shape in the 650−980 nm region where **1(c)** in the ground state has no absorption and only the positive absorption signal was observed in transient spectra.

The spectrum at 30 ps shows that rather broad absorption is overlapped on the spectral band observed at 0 ps, indicating that some additional species was produced in the condition with the higher excitation intensity. As shown in Figure 6c and d where the absorption spectra at 0 and 30 ps under the lower and higher excitation condition were respectively normalized,

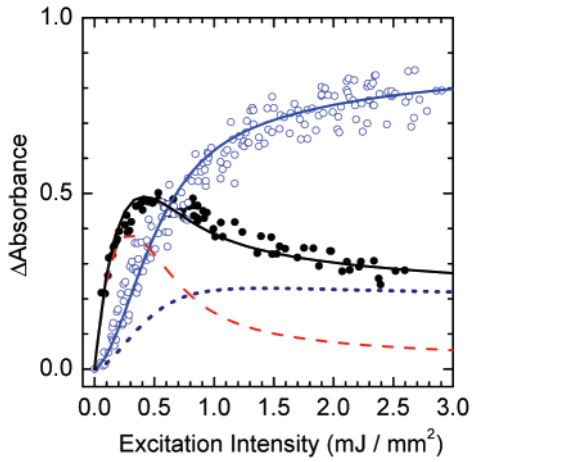

Figure 7. Excitation intensity dependence of transient absorbance of **1(c)** in *n*-hexane, observed at 20 ps, 580 nm (blue ○), and 20 ps, 900 nm (●), excited with a 15 ps 532 nm laser pulse. Lines in the figure are the calculated curves with the parameter set 1 in Table 2 (see text).

this broad positive absorption did not appear at 0 ps and was remarkable at 30 ps. It should be mentioned that this species completely decreased with increasing delay time after the excitation as shown in Figure 2. Because the time constant of the decay was not dependent on the monitoring wavelength of the positive band in the higher excitation condition in Figure 2, the lifetime of this transient species could be estimated to be ≤10 ps.

Mechanisms of the Enhancement of the Cycloreversion Reaction under the Picosecond Laser Pulse Excitation. To more precisely explore the drastic enhancement of the cycloreversion reaction under the picosecond laser excitation, the excitation intensity dependence on the transient absorption signals was investigated. Figure 7 shows the result at 20 ps after the excitation. The transient absorbance at 900 nm, due to the excited state of **1(c)**, increased consistently with the excitation intensity in the region where the excitation intensity is rather low, while further increase of the excitation intensity led to the decrease of the transient absorbance. Because the ground-state bleaching monitored at 580 nm monotonically increased with increasing excitation intensity, the decrease of the excited state in high excitation intensity is not attributable to the deactivation to the ground state but to the cycloreversion reaction.

Actually, at 160 ps at which the cycloreversion reaction was finished, the increase in the reaction efficiency with increasing excitation intensity was confirmed as shown in Figure 8. Here, the ordinate is given as the conversion efficiency defined as ΔA at 580 nm at 160 ps following the excitation divided by the absorbance of **1(c)** at 580 nm before the laser excitation. The unity of the conversion efficiency means that all of **1(c)** in the exposed volume is converted to **1(o)** by the laser irradiation. In the region where the excitation intensity is low, the slope of the reaction efficiency in Figure 8 is ca. 1.8, indicating that the two-photon absorption process is responsible for the cycloreversion.

Prior to the quantitative discussion on the simulated results shown by lines in Figures 7 and 8, it should be mentioned here that a less efficient nonlinear ring-opening process was observed under the femtosecond excitation. Usually, the two-photon absorption process can be divided into two classes such as a simultaneous process and a stepwise process. In the former

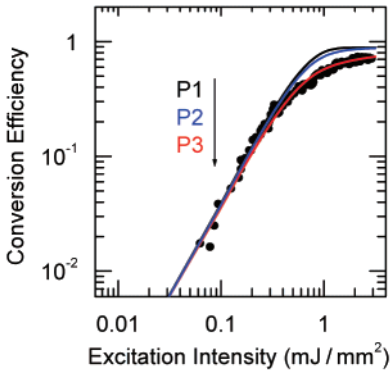

Figure 8. Excitation intensity dependence of the conversion efficiency of **1(c)** in *n*-hexane, observed at 160 ps after the excitation with a 15 ps, 532 nm laser pulse. Lines are calculated curves on the basis of the parameter set shown in Table 2; set 1 (P1, black line), set 2 (P2, blue line), and set 3 (P3, red line).

Table 1. Specifications of the Laser Systems

LASER	wavelength	pulse width (fwhm)	output/ pulse	peak energy	peak energy/ area size
PS (Nd^{3+}:YAG)	532 nm	15 ps	0.5−1.0 mJ	6.7×10^7 W (1 mJ)	$\sim 7 \times 10^9$ W/cm^2
FS (OPA/ Ti:Sapphire)	540−610 nm	150 fs	5−15 μJ	6.7×10^7 W (10 μJ)	$\sim 7 \times 10^{10}$ W/cm^2
ratio	comparable	1/100	1/100	1	10

simultaneous absorption process, the ground-state molecule is excited via simultaneous two-photon absorption even in the wavelength region where the molecule has no ground-state absorption. The number of the molecules excited by the simultaneous two-photon absorption is represented by eq 1.

$$N_e = \delta \cdot N_g \cdot I^2 \quad (1)$$

Here, δ and N_g are two-photon absorption cross-section and the number of the ground-state molecules, respectively. I is the peak intensity of the excitation pulse with the unit of the number of photon divided by unit area size and the time, typically given as photon number cm^{-2} s^{-1}.

On the other hand, the latter stepwise two-photon absorption process takes place in such a manner that the transient species produced by the first one-photon absorption by the ground-state molecule again absorbs the second photon resulting in the production of higher excited states. Because the second-photon absorption by the transient species occurs in competition with the first-photon absorption by the ground-state molecule, the number of the photon in a laser pulse is an important factor for the stepwise two-photon absorption process. Although the N_e is also in proportion with I^2 in the stepwise absorption process, the saturation tendency is pronounced with increasing excitation intensity. That is, under the condition that most of the ground state was pumped up to the S_1 state in the high excitation intensity region, the production of the S_n state via the absorption of the second photon was considered as a one-photon process.

The specification of the excitation lasers listed in Table 1 indicates that both the output energy per pulse and the pulse duration of the picosecond laser are almost 100 times larger than those of the femtosecond laser pulse and the peak intensities of these two laser outputs are almost comparable with each other. By taking the focusing area size into account, the peak intensity corresponding to I in eq 1 under the femtosecond laser excitation condition is ca. 10 times larger than that by the picosecond laser excitation. Hence, we can safely conclude that the stepwise two-photon process via the actual intermediate S_1 state, rather than the simultaneous two-photon process, was responsible for the enhancement of the cycloreversion process under the picosecond laser excitation. Actually, the decrease in the transient absorbance due to the excited state of **1(c)** in a rather high excitation intensity in Figure 6 directly supports the stepwise absorption process of the excited state.

Scheme 3

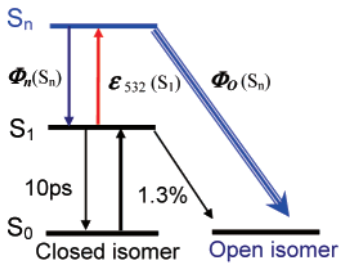

Numerical Computer Simulation for the Multiphoton Cycloreversion Reaction. To quantitatively estimate the cycloreversion reaction yield in the higher excited state attained by the second-photon absorption, we employed the computer numerical simulation based on Scheme 3, where several parameters for the simulation are indicated as italic styles such as ϵ_{532} (S_1), Φ_n (S_n), and Φ_o (S_n). Here, ϵ_{532} (S_1), Φ_n (S_n), and Φ_o (S_n) are respectively the extinction coefficient of the S_1 state of **1(c)** at 532 nm, the yield leading to the S_1 state from the higher excited state (S_n) attained by the second-photon absorption, and the cycloreversion reaction yield at the S_n state.

Although the estimation of the extinction coefficient of transient species is generally difficult, the overlap of the absorption band of the ground-state molecule on the transient absorption provides a rather rational estimation of the ϵ_{532} (S_1) value in the present case. The transient absorption spectrum is in general given as the Δabsorbance that is in proportion to ($\epsilon_e - \epsilon_g$) $\times$ C_e in the condition where the C_e value is the same as the bleaching concentration of the ground-state molecules. Here, ϵ_e, ϵ_g, and C_e are respectively the extinction coefficient of the excited-state molecule, that of the ground-state molecule, and the concentration of the excited-state molecule. The transient absorption spectrum immediately after the excitation with weak excitation intensity as shown in Figure 5 showed the negative absorbance at 532 nm. Because the open-form is not yet produced immediately after the excitation and the transient absorbance can be regarded as ($\epsilon_e - \epsilon_g$) $\times$ C_e, the negative absorbance indicates that the ϵ_{532} (S_1) value is smaller than that of **1(c)** in the ground state at 532 nm, 11 000 M^{-1} cm^{-1}. In addition, the transient absorption signals around 505 nm in the figure under the weak excitation condition are almost zero, indicating that the extinction coefficient of the excited state of **1(c)** is almost the same as that of the ground state (ca. 6000 M^{-1} cm^{-1}). Because the spectral band shape of the dip due to the bleaching of the ground state **1(c)** in Figure 6a and c under the weak excitation condition is almost the same as the negative image of the absorption spectrum of **1(c)**, it could be concluded that the absorption spectrum of the excited **1(c)** has no sharp structure around 500−550 nm. Hence, we could estimate that the extinction coefficient, ϵ_{532} (S_1), is ca. 6000 M^{-1} cm^{-1}.

In the actual calculation, we carried out the numerical simulation by using the ϵ_{532} (S_1) values of 3000, 6000, and 9000

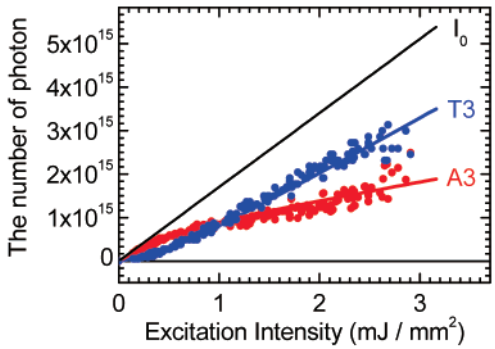

Figure 9. Excitation intensity dependence of the relation between the incident energy of a 15 ps, 532 nm laser pulse and the transmitted photon number (blue ●). The absorbed photon number (red ●) in the **1(c)** (7.5×10^{-5} M) in *n*-hexane solution is the value obtained by the subtraction of the transmitted photon number from the incident light energy (the curve of I_0). The curves T3 and A3 are calculated results for the transmitted light energy (*T*) and the adsorbed light energy (*A*) with parameter set 3 in Table 2.

M^{-1} cm^{-1} to confirm the effect of the ϵ_{532} (S_1) on the cycloreversion reaction yield Φ_o (S_n). Hence, the most important variable parameters are Φ_n (S_n) and Φ_o (S_n). To more quantitatively check the validity of the numerical simulation, we measured the incident and transmitted intensities of the picosecond 532 nm laser pulse as a function of the excitation intensity, as indicated in Figure 9. The numerical simulation was performed in such a manner that parameters chosen for the fitting of the experimental results in Figures 7 and 8 simultaneously can reproduce the experimental results shown in Figure 9.

First, we concentrate our discussion in Figure 8 where the excitation intensity dependence of the conversion efficiency of **1(c)** to **1(o)** was plotted as a function of the excitation intensity. In this figure, three lines with different parameter sets were plotted. The line P1 (smooth line) is the result calculated with the parameter set 1 where Scheme 3 was assumed and the cycloreversion yield, Φ_o (S_n), and the internal conversion yield to S_1 state, Φ_n(S_n), from the higher excited state (S_n) were respectively set to be 0.5 and 0.5. In addition, the lifetime of the S_n state was assumed to be zero or much shorter than the time interval of the numerical integration (0.1 ps). Although the calculated curve reproduced the experimental result in the region where the excitation intensity is <ca. 0.4 mJ/mm^2, the deviation between the experimental results and the calculated curve was pronounced with a further increase in the excitation intensity. The contribution of the lifetime in the higher excited state to the deviation was quantitatively elucidated by the calculation with the parameter set 2 in which the lifetime of the S_n state was assumed to be 2 ps. It should be noted that the lifetime of the higher excited state is usually in the order of subpicoseconds and the value of 2 ps is an exaggerated one to elucidate the contribution of the finite lifetime of the S_n state. Although the curve thus calculated as a broken line (curve P2) slightly shows a saturation tendency in high excitation regions, the large deviation is still observed between the experimental and calculated results. This result indicates that the lifetime of the S_n state is not a major factor for the saturation tendency in the experimental result.

In the explanation of Figure 6, we pointed out that some new transient species was produced under the high excitation intensity. Because this transient species was observed at 30 ps and was not detected at 0 ps in the excitation condition with 0.4 mJ/mm^2, this new species is produced after the second-photon absorption of the S_1 state. To take the contribution of this transient species into account, we have adopted Scheme 4 where the reaction pathway to the S_1' state from the S_n state was included. In addition, this S_1' state was assumed not to undergo the effective cycloreversion reaction upon the excitation to a higher electronic state. The extinction coefficient and the lifetime of the S'_1 state were respectively set to be identical to those of the S_1 state that can undergo the effective cycloreversion reaction in the higher excited state. The calculated result based on Scheme 4 (parameter set 3 in Table 2) is shown as a bold line (P3) in Figure 8, indicating that the calculated result well reproduces the experimental results in the entire excitation intensity region.

In addition, the simulation result thus calculated also reproduces the relation between the incident energy and the transmitted photon number in Figure 9 where the energy transmitted through the sample was measured as a function of the incident energy of the excitation picosecond 532 nm laser pulse into the sample. The ordinate is given as the number of the photon. The dotted line (I_0) is the simple relation between the excitation intensity and the number of the photon at 532 nm. Closed circles are the experimental results of the transmitted light energy, and open circles indicate the absorbed light energy obtained by the subtraction of the number of the absorbed photon from the dotted line I_0. The solid lines, T3 and A3, are the results with the parameter set 3 assuming the presence of the S_1' state that does not undergo the cycloreversion reaction in the higher excited state. The calculated curves well reproduce the experimental results in the entire region of the incident excitation intensity. The reproduction of the conversion efficiency in Figure 8 and the number of the absorbed photon in Figure 9 by the same parameter set leads to the conclusion that the two-photon absorption process into the S_n state resulting in the open-form isomer is in competition with the absorption process by some transient species as noted by the S_1' state produced by the internal conversion from the S_n state.

Table 2. Parameter Sets for the Simulation

	set 1	set 2	set 3
Φ_o (S_1)	0.013	0.013	0.013
τ (S_1)/ps	10	10	10
ϵ_{532} (S_0)/M^{-1} cm^{-1}	11 000	11 000	11 000
ϵ_{532} (S_1)/ M^{-1} cm^{-1}	6000	6000	6000
Φ_o (S_n)	0.5	0.5	0.5
Φ_n (S_n)	0.5	0.5	0
Φ_n' (S_n)	0	0	0.5
τ (S_n)/ps	0	2	0
Δt/ps	0.1	0.1	0.1
$\Delta l/\mu$m	10	10	10

Scheme 4

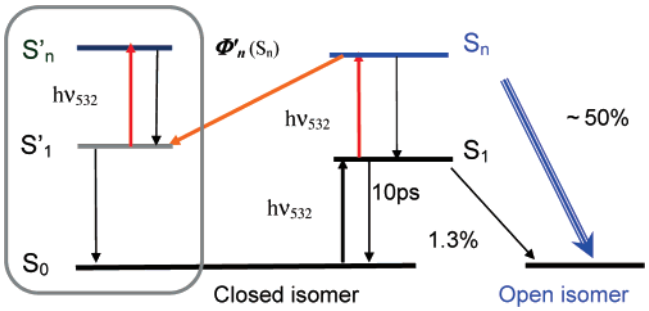

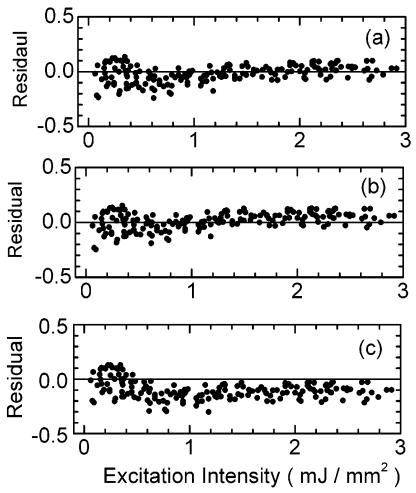

Figure 10. Weighted residual values between the experimental and the calculated results of excitation intensity dependence of the conversion efficiency of **1(c)** in *n*-hexane, observed at 160 ps after the excitation with a 15 ps, 532 nm laser pulse. Parameters used for the calculation were as follows: (a) parameter set 3 ($\epsilon_{532}(S_1) = 6000\ M^{-1}\ cm^{-1}$, $\Phi_o(S_n) = 0.5$, and $\Phi_n'(S_n) = 0.5$); (b) $\epsilon_{532}(S_1) = 9000\ M^{-1}\ cm^{-1}$, $\Phi_o(S_n) = 0.4$, and $\Phi_n'(S_n) = 0.6$; (c) $\epsilon_{532}(S_1) = 3000\ M^{-1}\ cm^{-1}$, $\Phi_o(S_n) = 0.6$, and $\Phi_n'(S_n) = 0.4$.

The excitation intensity dependence of the transient species of the S_1 and S_1' states was also analyzed by the numerical simulation with the parameter set 3 in Table 2. As was shown in Figure 7, the transient absorbance ascribed to the excited state of **1(c)** decreased with increasing excitation intensity in rather high intensity of the incident picosecond laser light. The broken and dotted lines in Figure 7 are calculated results for the contribution from the S_1 state and that from the S_1' state, respectively, and the solid line was obtained by the summation of the contributions from both of the excited states. In this summation, the extinction coefficient of the S_1' state is 1.2 times larger than that of the S_1 state. The calculated solid curve well reproduced the experimental result, showing the decrease of the excited states with increasing excitation intensity. In addition, the solid line for the transient absorbance at 580 nm, which is due to the bleaching of the S_0 state of **1(c)** at 20 ps, also reproduced the experimental results by the parameter set 3.

In any case, it is worth noting here that the calculated curves without the contribution from the S_1' state reproduced the experimental results shown in Figures 7−9 in rather low excitation intensity less than ca. 0.4 mJ/mm^2 where the contribution from the transient species noted as the S_1' state is very small. The above results indicate that the higher excited state produced by the second-photon absorption from the S_1 state of **1(c)** has a large reaction yield, 50%, of the cycloreversion, although some ambiguity remains in the estimation of parameters such as the extinction coefficient of the excited state at 532 nm.

Thus, we performed the numerical calculation by changing the extinction coefficient of the S_1 state at 532 nm, ϵ_{532} (S_1) for the reproduction of the experimental results, as mentioned in the beginning of this section. The excitation dependence in Figure 8 was analyzed by using different values of ϵ_{532} (S_1). The weighted residual, *r*, values between the experimental results, *Z*, and calculated results, *F*, were exhibited in Figure 10. The weighted residual value is given as $r_i = (Z_i - F_i)/\sqrt{Z_i}$. Although the deviation between the experimental results and the calculated curve was observed in the region of high excitation intensity, the values of 3000 and 9000 $M^{-1}\ cm^{-1}$ for ϵ_{532} (S_1) reproduced the experimental results in the region of rather low excitation intensity. For the low excitation region, the cycloreversion reaction yield in the higher excited state, $\Phi_o(S_n)$, was estimated to be 60% for ϵ_{532} (S_1) = 3000 $M^{-1}\ cm^{-1}$ and 40% for ϵ_{532} (S_1) = 9000 $M^{-1}\ cm^{-1}$. By taking into account the possibility of some other nonlinear processes in the high excitation intensity region and the uncertainty of the extinction coefficient of the excited state at 532 nm, we may conclude that higher excited state has a rather high cycloreversion yield as (50 ± 10)%. Summarizing the above results and discussion, it can be concluded that the drastic enhancement in the cycloreversion efficiency under the picosecond 532 nm laser excitation is ascribed to the large reaction yield in the higher excited state attained by the second-photon absorption.

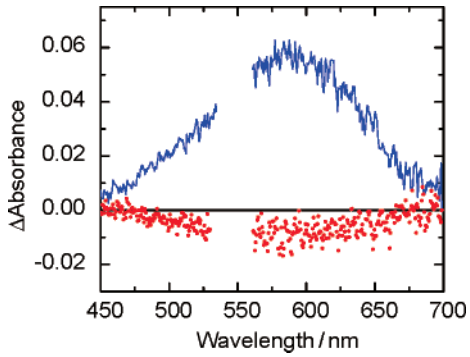

Figure 11. Difference absorption spectra of **1** (**1(c)** 85% and **1(o)** 15%) in *n*-hexane solution observed at 100 ns after the excitation with a 5 ns laser pulse with 0.1 mJ/mm^2 output power. Excitation wavelength for the red dotted line and that for the blue solid line were 532 and 266 nm, respectively.

Comparison of the Cycloreversion by the 532 nm Two-Photon Absorption to That by the 266 nm One-Photon Absorption. On the properties of the S_1' state, it is worth mentioning a recent theoretical investigation on the excited state of the diarylethene system,[30,31] predicting that the excited state optically forbidden from the S_0 state locates in the vicinity of the optically allowed S_1 state. Although the production of this state is not allowed by the direct excitation from the S_0 state, it may possibly be generated via internal conversion from higher S_n excited state. Provided that the selection rule of the optical absorption is applicable to the present **1(c)** molecule, the higher excited state produced via the absorption by the S_1' state is also optically allowed from the S_0 state. To elucidate the characters of the S_1' and S_n' states, we measured the reaction profiles by the excitation at 266 nm. In this experiment, we employed the nanosecond laser pulse with long pulse duration, because the nanosecond laser has a long pulse duration (ca. 5 ns) as compared to the lifetime of the S_1 state and the effective multiphoton absorption process can be negligible. The cycloreversion reaction yield under a nanosecond 532 nm laser pulse excitation of **1(c)** in *n*-hexane solution as shown by the red line in Figure 11 was ca. 1% and was in consistent with that under steady-state light irradiation (1.3%).

(30) Uchida, K.; Guillaumont, D.; Tsuchida, E.; Mochizuki, G.; Irie, M.; Murakami, A.; Nakamura, S. *J. Mol. Struct.* (*THEOCHEM*) **2002**, *579*, 115.
(31) Guillaumont, D.; Kobayashi, K.; Kanda, K.; Miyasaka, H.; Uchida, K.; Kobatake, S.; Shibata, K.; Nakamura, S.; Irie, M. *J. Phys. Chem. A* **2002**, *106*, 7222.

The spectrum observed at 100 ns after the excitation at 266 nm in Figure 11 shows the production of the closed-form. Because the solution contains both **1(c)** (85%) and **1(o)** (15%), the difference of the population of **1(c)** and **1(o)**, ΔN, is represented by the following eq 2.

$$\Delta N = \left(\frac{\epsilon_O^{266} C_O}{\epsilon_O^{266} C_O + \epsilon_C^{266} C_C} \Phi_{O \rightarrow C}^{266} - \frac{\epsilon_C^{266} C_C}{\epsilon_O^{266} C_O + \epsilon_C^{266} C_C} \Phi_{C \rightarrow O}^{266} \right) \cdot I_0 \quad (2)$$

Here, C_O, C_C, ϵ_O^{266}, and ϵ_C^{266} are respectively the concentration and the extinction coefficient of **1(o)** and **1(c)**. The values $\Phi_{O \rightarrow C}^{266}$ and $\Phi_{C \rightarrow O}^{266}$ are respectively the reaction yield of the cyclization and that of the cycloreversion at 266 nm excitation. I_0 represents the number of the photon absorbed by the system and the number of the total incident photon at 266 nm, and the concentration of the photon is 2.2×10^{-5} M. Here, ΔN is defined as a positive value for the case that the population of **1(c)** increases. The ratios C_O/C_C and $\epsilon_O^{266}/\epsilon_C^{266}$ are 0.15/0.85 and 2.1/1, respectively. Provided that all of the photon is absorbed and the cyclization yield of $\Phi_{O \rightarrow C}^{266}$ is the same as that obtained under the steady-state light irradiation (0.59), we could estimate the cycloreversion yield, $\Phi_{C \rightarrow O}^{266}$, on the basis of the change of the absorption in Figure 11. The increase of the **1(o)** state in the above experimental condition with the $\Phi_{O \rightarrow C}^{266}$ value of 0.59 led to the estimation of the $\Phi_{C \rightarrow O}^{266}$ value to be ca. 1%. In other words, the $\Phi_{C \rightarrow O}^{266}$ value could be estimated to be less than a few % even in the case that the cyclizations yield $\Phi_{O \rightarrow C}^{266}$ is unity. The small cycloreversion yield also assists the presence of the S_1' state with a small cycloreversion reaction yield in the higher excited state attained by one more photon absorption under the picosecond laser excitation. The above results indicate that the production of higher electronic excited states does not directly lead to the effective cycloreversion reaction and that the character of the electronic state takes an important role in the reaction.

Although several theoretical studies have been published on the photochromic reaction of diarylethene derivatives,[18,19,30−33] most of them concentrated their attention on the lowest or lower excited states. In addition, precise calculation with quantitative reliability is still difficult for higher excited states of large molecular systems such as diarylethene derivatives. Recent investigation[31] by Guillaumont et al. reported that the lower barrier for the cycloreversion reaction is attained in higher excited states. In addition, it was pointed out that these states are optically forbidden states from the ground state. This result supports the present experimental result that the successive two-photon absorption opens the effective cycloreversion reaction in the higher excited state. The difference in the reactivity between one- and two-photon absorption processes suggests that the symmetry of the electronic states takes an important role in the cycloreversion in the higher excited state.

Concluding Remarks

Picosecond pulsed excitation of the closed-isomer of the diarylethene derivatives led to the drastic enhancement of the cycloreversion reaction. The dependence of the reaction profiles on the excitation intensity, pulse duration, and the excitation wavelength indicated that this enhancement is attributable to the production of the higher excited state with a large reaction yield of the cycloreversion (50 ± 10)% attained via a successive two-photon process. Comparison of the reaction yield by one-photon absorption to higher excited states to that via the successive two-photon process showed that not the energy of the incident light but the character of the excited electronic state is of crucial importance for the efficient cycloreversion reaction to take place. The relation between the character of the electronic state and the reaction yield in the higher excited state is now under investigation.

Finally, it is worth pointing out here that the present excitation condition of ca. mJ/mm^2 is equal to the intensity of nJ/μm^2 that can be attainable by the combination use of the diode picosecond visible laser and a microscope. We anticipate that the present result will provide a new approach for one-color light control of the gated photochromic system, which can be utilized for an erasable memory system with nondestructive readout capability.

Acknowledgment. We thank Dr. S. Nakamura from the Mitsubishi Chemical Corp. for valuable discussions. This work was partly supported by Grant-in-Aids for Scientific Research on Priority Areas (417) (No. 15033242) and (No. 16350012) from the Ministry of Education, Culture, Sports, Science, and Technology (MEXT) of the Japanese Government.

JA049177+

(32) Nakamura, S.; Irie, M. *J. Org. Chem.* **1988**, *53*, 613.
(33) Boggio-Pasqua, M.; Ravaglia, M.; Bearpark, M. J.; Garavelli, M.; Robb, M. A. *J. Phys. Chem. A* **2003**, *107*, 11139.